CrossMark

ORIGINAL PAPER

Modeling and analyses of driver's characteristics in a traffic system with passing

Sapna Sharma

Abstract This paper investigates the effect of aggressive or timid characteristics of driver's behavior with passing by means of lattice hydrodynamic traffic flow model. The effect of driver's characteristic on the stability of traffic flow is examined through linear stability analysis. It is shown that for both the cases of passing or without passing the stability region significantly enlarges (reduces) as the proportion of aggressive (timid) drivers increases. To describe the propagation behavior of a density wave near the critical point, nonlinear analysis is conducted and mKdV equation representing kink–antikink soliton is derived. It is observed that jamming transition occurs between uniform flow and kink jam phase with increase in aggressive driver's characteristics for smaller values of passing. When passing constant is greater than a critical value, jamming transitions occur among uniform traffic flow and kink-Bando traffic wave through chaotic phase. Numerical simulation is carried out to validate the theoretical findings which confirm that traffic jam can be suppressed efficiently by considering the driver's characteristics in a single-lane traffic system with or without passing.

Keywords Traffic flow · Driver's characteristics · mKdVs equation · Lattice model

S. Sharma (✉)
School of Mathematics, Thapar University, Patiala, Punjab 147004, India
e-mail: sapna2002@gmail.com

1 Introduction

In today's era, traffic congestion is a serious issue due to the rapid increase in automobiles on road throughout the world. Due to which, the complexity involved in traffic flow problems attracted the attention of scientists and researchers. Traffic congestion not only increases energy consumption and emissions but it also imposes safety hazards. From the last few decades various traffic models, such as car-following models, cellular automaton models, lattice hydrodynamic models, gas-kinetic models, and fluid-dynamic models, have been developed to understand the dynamics of traffic flow and investigate the properties of traffic jams [1–28]. Among them, the lattice hydrodynamic model firstly proposed by Nagatani [10], which incorporates the idea of the microscopic optimal velocity model, is one of the convenient model for analyzing the density wave in traffic flow. In this approach, traffic congestion is represented in terms of kink density wave through Modified Korteweg–de Vries (mKdV) equation. Subsequently, this modeling approach was widely referred and extended to study various nonlinear phenomenon present in vehicular traffic flow like backward effect [12], lateral effect of the lane width [13], anticipation effect of individual driving behavior [14], and explicit driver's physical delay [15].

In real traffic, the driver always adjusts his/her velocity according to observed traffic situation in the surroundings and estimates his/her driving behavior. To capture this complex phenomenon, few efforts [17,18,

20,27,28] have been made in the past. In this direction, Sharma [27] recently analyzed the behavior of driver characteristic on a two-lane traffic flow phenomena. To incorporate one of the important traffic characteristics, Nagatani [10] extended his model to take into account the passing effect in one-dimensional traffic flow phenomena. Later, Gupta and Redhu [23] analyzed the passing effect with driver anticipation effect on traffic flow and concluded that passing parameter is an important parameter which plays an important role to stabilize traffic flow. As seen in real traffic on highways, both the above-mentioned traffic phenomena are interconnected as aggressive drivers try to move fast due to which overtaking takes place. Therefore, it will be more adequate to investigate the driver's characteristic with the consideration of passing. This motivates us to develop a lattice model by incorporating the effect of driver's behavior with passing.

In this paper, a more realistic uni-dimensional lattice hydrodynamic traffic flow model is presented with the consideration of driver's behavior and passing is allowed in the traffic system. The rest of the paper is organized as follows: In Sect. 3, the stability condition of traffic flow is derived by means of linear stability theory. To describe the propagation behavior of traffic jams, Sect. 4 is devoted to the nonlinear analysis in which mKdV equation is computed near the critical point. Numerical simulations are carried out to validate the theoretical findings in Sect. 5, and finally, conclusions are drawn in Sect. 6.

2 A new LH model

The first lattice hydrodynamic model for vehicular traffic that describe the traffic phenomena on an unidirectional single-lane highway, is proposed by Nagatani [10], is given as

$$\partial_t \rho_j + \rho_0(\rho_j v_j - \rho_{j-1}v_{j-1}) = 0, \tag{1}$$
$$\partial_t(\rho_j v_j) = a[\rho_0 V(\rho_{j+1}) - \rho_j v_j]. \tag{2}$$

where ρ_0 is the average density and sensitivity $a = 1/\tau$ corresponds to the inverse of delay time (τ); ρ_j and v_j, respectively, represent the local density and velocity at site j at time t. $V(.)$ is the optimal velocity function which is a monotonically decreasing function having an upper bound and an inflection point at critical density. In this model, the variation in traffic flow ρv at site j is

determined by the difference between the actual flow at site j and the optimal flow $\rho_0 V(\rho_{j+1})$ at the next site $j + 1$.

The optimal velocity function adopted by Nagatani [19] is used.

$$V(\rho) = \frac{V_{\max}}{2}\left[\tanh\left(\frac{1}{\rho} - \frac{1}{\rho_c}\right) + \tanh\left(\frac{1}{\rho_c}\right)\right], \tag{3}$$

where $V_{\max}$ and ρ_c denote the maximal velocity and the safety critical density, respectively. The optimal velocity function is monotonically decreasing, and has an upper bound and a turning point at $\rho = \rho_c = \rho_0$. For computation purpose, maximal velocity and critical density are set at 2.0 and 0.25, respectively.

To mimic the traffic dynamics more realistically, Nagatani [10] further extended the lattice model by incorporating the effect of passing in to evolution equation while Eq. (1) representing the conservation of vehicles remain unaltered. It was considered that when the traffic current on site j is greater than the traffic current on site $j + 1$ then passing takes place and is proportional to the difference between the optimal current at site j and $j + 1$.

$$\partial_t(\rho_j v_j) = a[\rho_0 V(\rho_{j+1}(t)) - \rho_j v_j] \\ + a\gamma[\rho_0 V(\rho_{j+1}(t)) - \rho_0 V(\rho_{j+2}(t))]. \tag{4}$$

where γ is a passing constant. Later, Gupta and Redhu [23] modified the Nagatani's model to analyze the effect of driver's anticipation with passing.

Recently, driver's behavior which plays an important role on traffic flow dynamics has been given much attention [23,27,28]. In general, drivers behavior can be characterized in three equilibrium states, i.e, aggressive, normal or timid. In real traffic, aggressive drivers drive faster while the timid drivers drive slower as compared to the normal drivers and influences the traffic flow to a larger extent. Aggressive drivers always overestimate the downstream density by observing intervehicular space that is shorter than the equilibrium spacing while timid drivers often underestimate it. This influences the driver's perceived optimal velocity. To capture the effect of driver's characteristics, a lattice hydrodynamic model in a two-lane system is developed [27]. A modified evolution equation is proposed by incorporating a parameter p to reflect the influence of driver's characteristics with the consideration of anticipation driving effect as follows:

$$\partial_t(\rho_j(t)v_j(t)) = a\rho_0[V(\rho_{j+1}(t)) + \alpha(2p-1)$$
$$\times \tau V'(\rho_{j+1}(t))\partial_t(\rho_{j+1}(t))] - a\rho_j(t)v_j(t). \quad (5)$$

where α is the anticipation coefficient corresponds to driver's behavior. For timid drivers, the positive value of α corresponds to the explicit driver's physical delay in sensing perceived optimal velocity. Here, the bigger value of α corresponds to more skillful aggressive drivers in the model. When $\alpha = 0$, the new model reduces to Nagatani's [19] for normal drivers. The parameter $0 \le p \le 1$ represents the intensity of influence of drivers' characteristics in the traffic stream. Here, $p = 1$ represents the drivers aggressive characteristics in a traffic system with intelligent transportation system (ITS). Whereas $p = 0$ corresponds to the drivers timid characteristics which usually underestimate the optimal velocity. Though the above model is able to analyze the effect of drivers characteristics on a unidirectional road but cannot be applied to the traffic flow when passing is applied as the passing effect has not been considered. Therefore, we propose a new evolution equation by incorporating the effect of passing with the consideration of anticipation driving effect on a traffic flow system as follows:

$$\partial_t(\rho_j(t)v_j(t)) = a\rho_0[pV(\rho_{j+1}(t+\alpha\tau))$$
$$+ (1-p)V(\rho_{j+1}(t-\alpha\tau))]$$
$$- a\rho_j(t)v_j(t) + a\gamma[\rho_0 V(\rho_{j+1}(t+\alpha\tau))$$
$$- \rho_0 V(\rho_{j+2}(t+\alpha\tau))]. \quad (6)$$

For simplicity, using the Taylor series expansion and neglecting the non-linear terms, the new evolution equation can be obtained as:

$$\partial_t(\rho_j(t)v_j(t)) = a\rho_0[V(\rho_{j+1}(t)) + \alpha(2p-1)$$
$$\times \tau V'(\rho_{j+1}(t))\partial_t(\rho_{j+1}(t))] - a\rho_j(t)v_j(t)$$
$$+ a\gamma\rho_0[[V(\rho_{j+1}(t) - V(\rho_{j+2}(t)]$$
$$+ \alpha\tau[V'(\rho_{j+1}(t))\partial_t(\rho_{j+1}(t))$$
$$- V'(\rho_{j+2}(t))\partial_t(\rho_{j+2}(t))]]. \quad (7)$$

By taking the difference form of Eqs. (1) and (7) and eliminating speed v_j, the density evolution equation is obtained as

$$\rho_j(t+2\tau) - \rho_j(t+\tau) + \tau\rho_0^2[V(\rho_{j+1}(t))$$
$$- V(\rho_j(t))] + \tau\gamma\rho_0^2[2V(\rho_{j+1}(t))$$

$$- V(\rho_j(t)) - V(\rho_{j+2}(t))]$$
$$+ \alpha\rho_0^2\tau(2p-1)[V'(\rho_{j+1}(t))\tilde{\Delta}\rho_{j+1}(t)$$
$$- V'(\rho_j(t))\tilde{\Delta}\rho_j(t)]$$
$$+ \tau\alpha\gamma\rho_0^2[2V'(\rho_{j+1}(t))\tilde{\Delta}\rho_{j+1}(t)$$
$$- V'(\rho_{j+2}(t))\tilde{\Delta}\rho_{j+2}(t) - V'(\rho_j(t))\tilde{\Delta}\rho_j(t)] = 0. \quad (8)$$

Here $\Delta\rho_j(t) = \rho_{j+1}(t) - \rho_j(t)$ and $\tilde{\Delta}\rho_j(t) = \rho_j(t+\tau) - \rho_j(t)$.

3 Linear stability analysis

Linear stability analysis is being performed on the proposed model to investigate the influence of driver's characteristics on the jamming transition of traffic flow when passing is allowed. Under the condition of homogeneous traffic flow, the state of uniform traffic is represented by a constant density ρ_0 and optimal velocity $V(\rho_0)$. Hence, the steady-state solution of the homogeneous traffic flow on a two-lane highway is given as

$$\rho_j(t) = \rho_0, \quad v_j(t) = V(\rho_0). \quad (9)$$

Let $y_j(t)$ be a small deviation to the steady-state density on site j. Then,

$$\rho_j(t) = \rho_0 + y_j(t). \quad (10)$$

Inserting this perturbed density profile into Eq. (8) and linearizing it, we obtain

$$y_j(t+2\tau) - y_j(t+\tau) + \tau\rho_0^2 V'(\rho_0) \Delta y_j(t)$$
$$+ \alpha\tau\rho_0^2 V'(\rho_0)(2p-1)\tilde{\Delta}(\Delta y_j(t))$$
$$- \tau\gamma\rho_0^2 V'(\rho_0) \Delta^2 y_j(t)$$
$$- \alpha\gamma\tau\rho_0^2[V'(\rho_0) \Delta^2 \tilde{\Delta}y_j(t)] = 0. \quad (11)$$

Putting $y_j(t) = exp(ikj + zt)$ in Eq. (11), we get

$$e^{2\tau z} - e^{\tau z} + \tau\rho_0^2 V'(\rho_0)[e^{ik} - 1]$$
$$+ \alpha V'(\rho_0)(2p-1)[e^{\tau z} - 1][e^{ik} - 1]$$
$$- \tau\gamma\rho_0^2 V'(\rho_0)[e^{ik} - 1]^2$$
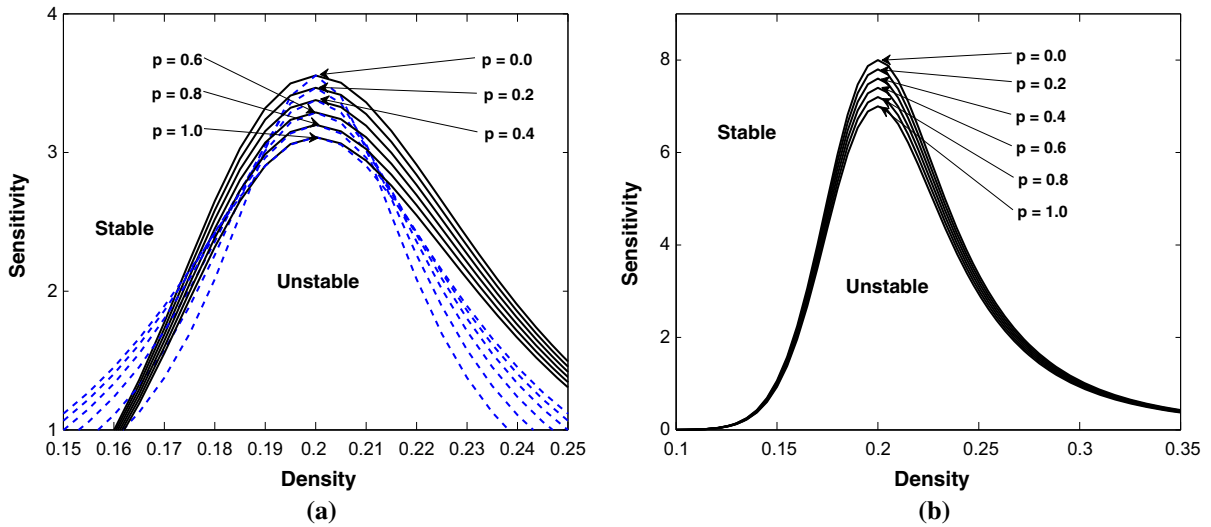$$- \alpha\tau\gamma\rho_0^2[e^{ik} - 1]^2[e^{\tau z} - 1] = 0. \quad (12)$$

Fig. 1 Phase diagram in parameter space (ρ, a), $\alpha = 0.1$ for **a** $\gamma = 0$, and **b** $\gamma = 0.1$, respectively

Substituting $z = z_1(ik) + z_2(ik)^2...$ into Eq. (12), we obtained the first- and second-order terms of the coefficient (ik) as

$$z_1 = -\rho_0^2 V'(\rho_0), \tag{13}$$

$$z_2 = -\frac{3\tau z_1^2}{2} - \frac{\rho_0^2 V'(\rho_0)}{2}$$
$$- \tau\alpha\rho_0^2 V'(\rho_0)(2p-1)z_1 + \gamma\rho_0^2 V'(\rho_0). \tag{14}$$

When $z_2 < 0$, the homogeneous steady-state flow becomes unstable for long-wavelength waves. While for $z_2 > 0$ the uniform flow becomes stable. Thus, the neutral stability condition for the steady-state is given as

$$\tau = -\frac{1 - 2\gamma}{\rho_0^2 V'(\rho_0)[3 - 2\alpha(2p-1)]}. \tag{15}$$

Thus the instability criterion for the homogeneous traffic flow is given as

$$\tau > -\frac{1 - 2\gamma}{\rho_0^2 V'(\rho_0)[3 - 2\alpha(2p-1)]}. \tag{16}$$

It is clear from Eq. (15) that parameters representing drivers' behavior p and passing effect γ play an important role on the stability of traffic flow in a single-lane traffic system. For $p = 1$, the above unstability condition (Eq. 15) reduces to the one obtained by Gupta and

Redhu [23]. The neutral stability curves in the phase space (ρ, a) are shown by solid curves in Fig. 1a, b for different parameter values. For a fix γ, Fig. 1a depicts the effect of p on stability corresponding to without passing, i.e., $\gamma = 0$ while Fig. 1b examines the similar effect corresponding to the passing case for $\gamma = 0.1$. It is observed that the apex of these curves (ρ_c, a_c) decreases with an increase in p in both the cases ensuring that larger value of p leads to enlargement in the stability region and hence, the traffic jam is suppressed efficiently. Moreover, on comparing Fig. 1a, b, it can also be concluded that under the similar conditions aggressive (timid) drivers have positive (negative) effect on the stability of traffic flow. It can be explained as in real traffic flow under the jam situation, aggressive drivers try to overtake if possible otherwise they try to accommodate themselves in a less denser lane by changing their lane quite frequently to overcome the congestion.

4 Nonlinear stability analysis

We investigate the effect of driver's behavior on the evolution characteristic of traffic jam around the critical point (ρ_c, a_c) on coarse-grained scales using reduction perturbation technique in this section. Long-wavelength expansion method is used to understand the slowly varying behavior near the critical point. For that, the slow variables X and T for a small positive

Table 1 The coefficients k_i of the model

k_1	k_2	k_3	
$b + \rho_c^2 V'$	$\frac{3}{2}b^2\tau + \rho_c^2 V'[\frac{1}{2} + b\alpha\tau(2p-1) - \gamma]$	$\frac{7}{6}b^3\tau^2 + \frac{\rho_c^2 V'}{6}[1 + 3\alpha(2p-1)b\tau(1+b\tau) - 6\gamma(1+\alpha\tau b)]$	
k_4	k_5	k_6	k_7
$\frac{\rho_c^2 V'''}{6}$	$3b\tau + \alpha\tau(2p-1)\rho_c^2 V'$	$\frac{5}{8}b^4\tau^3 + \frac{\rho_c^2 V'}{24}[1 + 6\alpha(2p-1)(b^2\tau^2 + \frac{2}{3}b^3\tau^3 + \frac{2}{3}b\tau) - 14\gamma - 12\alpha\gamma(b^2\tau^2 + 2b\tau)]$	$\frac{\rho_c^2 V'''}{12}$

Table 2 The coefficients g_i of the model

g_1	g_2	g_3
$-\frac{7}{6}b^3\tau_c^2 - \frac{\rho_c^2 V'}{6}[1 + 3\alpha b\tau_c(2p-1)(1+b\tau_c) - 6\gamma b\tau_c\alpha - 6\gamma]$	$\frac{\rho_c^2 V'''}{6}$	$\frac{3}{2}b^2\tau_c + b\alpha(2p-1)\tau_c\rho_c^2 V'$
g_4		g_5
$(3b + \alpha(2p-1)\rho_c^2)\tau_c g_1 + \frac{5}{8}b^4\tau_c^3 + \frac{\rho_c^2 V'}{6}[(\frac{-7\gamma}{12} + \frac{1}{4}) - \alpha\gamma(6b\tau_c + 3b^2\tau_c^2) + \alpha(2p-1)(b\tau_c + \frac{3b^2\tau_c^2}{2} + b^3\tau_c^3)]$		$\frac{\rho_c^2 V'''}{12} - [3b\tau_c + \alpha\rho_c^2\tau_c V'(2p-1)]g_2$

scaling parameter ϵ $(0 < \epsilon \ll 1)$ are defined as follows:

$$X = \epsilon(j + bt), \quad T = \epsilon^3 t, \tag{17}$$

where b is a constant to be determined. Let ρ_j satisfy the following equation:

$$\rho_j(t) = \rho_c + \epsilon R(X, T). \tag{18}$$

By expanding Eq. (8) using Taylor expansion up to fifth order (see "Appendix") of ϵ with the help of Eqs. (17) and (18), the following nonlinear equation is obtained.

$$\epsilon^2 k_1 \partial_X R + \epsilon^3 k_2 \partial_X^2 R + \epsilon^4(\partial_T R + k_3 \partial_X^3 R + k_4 \partial_X R^3) + \epsilon^5(k_5 \partial_T \partial_X R + k_6 \partial_X^4 R + k_7 \partial_X^2 R^3) = 0. \tag{19}$$

The coefficients k_i $(i = 1, 2, \ldots, 7)$ are given in Table 1, where $V' = \frac{dV(\rho)}{d\rho}|_{\rho=\rho_c}$, $V''' = \frac{d^3 V(\rho)}{d\rho^3}|_{\rho=\rho_c}$. Near the critical point (ρ_c, a_c), the value of τ is set as

$$\tau = \tau_c(\epsilon^2 + 1). \tag{20}$$

By taking $b = -\rho_c^2 V'$ and eliminating the second-order and third-order terms of ϵ, we obtain

$$\epsilon^4(\partial_T R - g_1 \partial_X^3 R + g_2 \partial_X R^3) + \epsilon^5(g_3 \partial_X^2 R + g_4 \partial_X^4 R + g_5 \partial_X^2 R^3) = 0, \tag{21}$$

where the coefficients g_i $(1, 2, \ldots, 5)$ are given in Table 2. To convert Eq. (21) into standard mKdV equation, the following transformations are adopted.

$$T' = g_1 T, \quad R = \sqrt{\frac{g_1}{g_2}} R'. \tag{22}$$

Then, Eq. (21) can be written as

$$\partial_T' R' - \partial_X^3 R' + \partial_X R'^3 + \epsilon M[R'] = 0, \tag{23}$$

where $M[R'] = \frac{1}{g_1}[g_3 \partial_X^2 R' + g_4 \partial_X^4 R' + \frac{g_1 g_5}{g_2} \partial_X^2 R'^3]$. After ignoring $O(\epsilon)$ correction term from Eq. (23), we get the solution of the standard mKdV equation as

$$R_0'(X, T') = \sqrt{c} \tanh\left(\sqrt{\frac{c}{2}}(X - cT')\right), \tag{24}$$

Here c is the propagation velocity for the kink–antikink solution and is computed by solving the following necessary condition:

$$(R'_0, M[R'_0]) \equiv \int_{-\infty}^{\infty} dX R'_0 M[R'_0] = 0, \qquad (25)$$

with $M[R'_0] = M[R']$. By solving Eq. (25), the selected value of c is

$$c = \frac{5g_2 g_3}{2g_2 g_4 - 3g_1 g_5}. \qquad (26)$$

Hence, the kink–antikink solution is given by

$$\rho_j = \rho_c + \epsilon \sqrt{\frac{g_1 c}{g_2}} \tanh\left(\sqrt{\frac{c}{2}}(X - cg_1 T)\right), \qquad (27)$$

with $\epsilon^2 = \frac{a_c}{a} - 1$ and the amplitude A of the solution is

$$A = \sqrt{\frac{g_1}{g_2}\epsilon^2 c}. \qquad (28)$$

The above kink solution exist only if the following condition is satisfied.

$$1 - 13\gamma - 14\gamma^2 + \alpha^2(5 - 12\gamma^2 + 12\gamma(-1 + p) - 6p)$$
$$+ 6\alpha(\gamma(7 - 5p) + 2(-1 + p) + 2\gamma^2(1 + p)) > 0. \qquad (29)$$

So the existence condition for kink solution is

$$0 \leq \gamma < f(\alpha, p). \qquad (30)$$

where

Fig. 2 Phase diagram in parameter space (γ, a)

is worthy to note that the coexisting and neutral stability curves divide the phase plane into stable, metastable and unstable region as shown in Fig. 1a. The traffic flow in the stable region will remain stable under a disturbance, while in metastable and unstable region, a small disturbance will lead to the congested traffic.

From Fig. 1, it is clear that with an increase in p, the corresponding neutral and coexisting curves both lower down, which indicates that the aggressive behavior of the driver can help in stabilizing the traffic flow. Additionally, the coexisting curves do not exist at $\gamma = 0.1$ for any value of p as the condition $\gamma < f(\alpha, p)$ is not satisfied (see Fig. 1b). Figure 2 shows the phase diagram in parameter space (γ, a) for different values of p. The curve $a_c = \frac{3 - 2\alpha(2p-1)}{1 - 2\gamma}$ for $\gamma < f(\alpha, p)$ rep-

$$f(\alpha, p) = \frac{13 + \alpha(30p - 42) + 12\alpha^2(1 - p) - (3 - 2\alpha)\sqrt{25 + (-168 + 156p)\alpha + (96 - 144p + 36p^2)\alpha^2}}{2(-14 + 12\alpha(1 + p) - 12\alpha^2)}. \qquad (31)$$

The mKdV equation (23) exists only for $0 \leq \gamma < f(\alpha, p)$ and cannot be derived from above nonlinear analysis for $\gamma \geq f(\alpha, p)$. For a particular case, when $\alpha = 0$ and $p = 1$, the existence condition for kink solution matches with the results obtained in Ref. [19]. Moreover, for $\gamma < f(\alpha, p)$, the kink–antikink solution of mKdV equation represents the coexisting phase which includes both congested phase and freely moving phase described by $\rho_j = \rho_c \pm A$ in the phase space(ρ, a). The coexisting curves obtained from nonlinear analysis are plotted by dashed lines in Fig. 1a. It
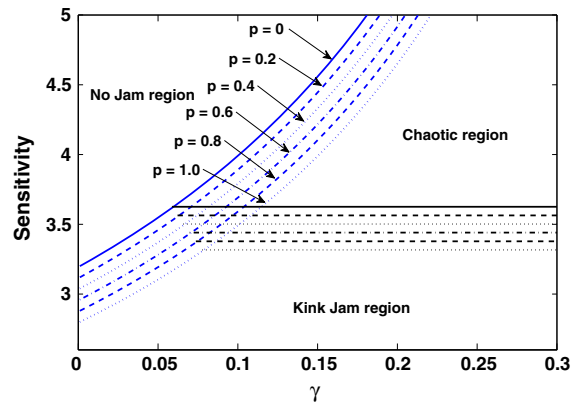
resents the phase boundaries between no jam and kink jam, while for $\gamma \geq f(\alpha, p)$, it represents the phase boundaries between no jam and chaotic region. It is clear from Fig. 2 that there exist only two regions no jam and kink jam in the phase diagram for $\gamma < f(\alpha, p)$. Moreover, the kink (no jam) region reduces (enhances) with an increase in the value of p. These results are in accordance with the findings of Ref. [24] that traffic jam can be suppressed efficiently by incorporating more aggressive drives in the traffic stream. For $\gamma \geq f(\alpha, p)$, i.e., when passing is high, based upon
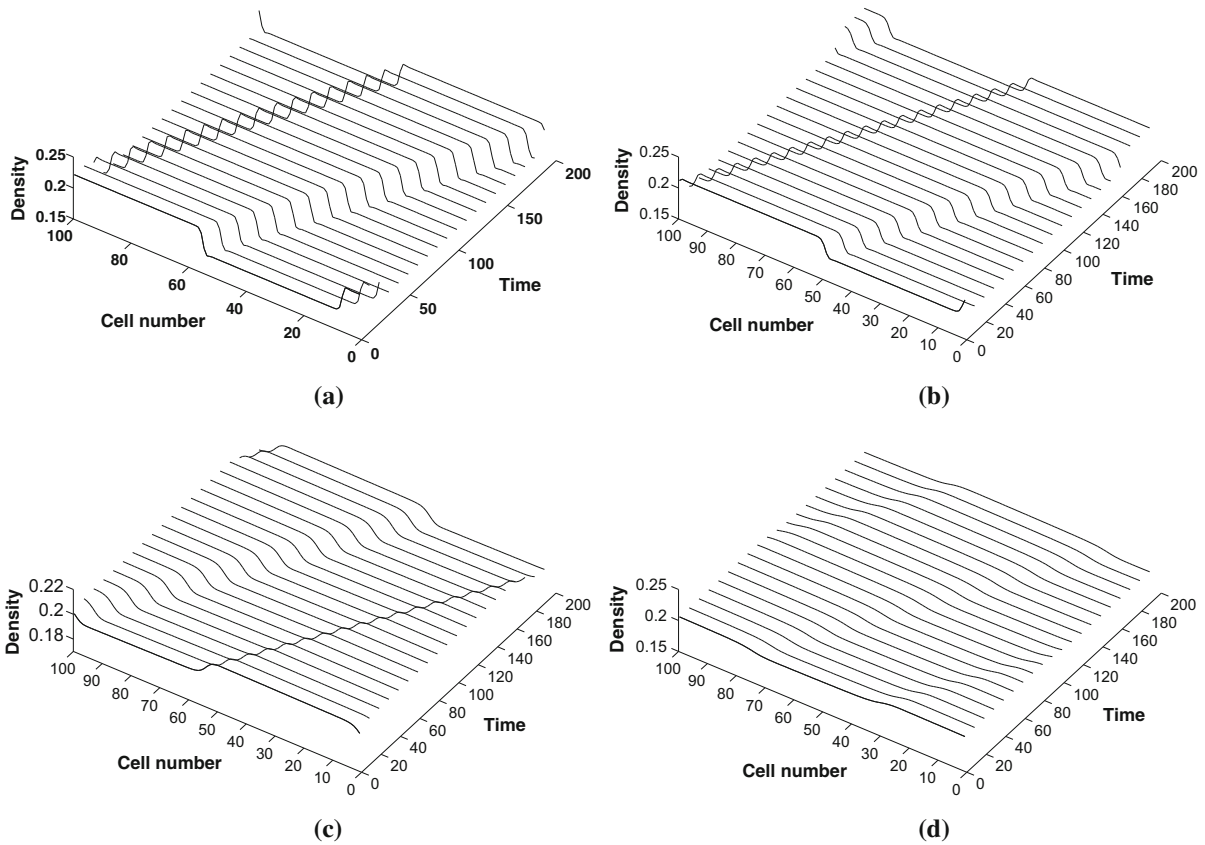
Fig. 3 Spatiotemporal evolutions of density when $\gamma = 0.05$, $\alpha = 0.1$, and $a = 3.2$ for **a** $p = 0$, **b** $p = 0.4$, **c** $p = 0.8$, and **d** $p = 1.0$, respectively

the kinds of density wave, the unstable region is further divided into two subregions: kink jam and chaotic jam. The boundary between kink and chaotic jam is the line $a = \frac{3-2\alpha(2p-1)}{1-2f}$. Similar to the previous case, in this case also the free flow region enhances while both the chaotic and kink jam regions reduce with an increase in the value of p.

5 Numerical simulation

Now, we carry out numerical simulation of the new model to investigate the effect of drivers characteristics with passing on traffic flow dynamic as well as to validate the theoretical results obtained by linear and nonlinear analysis in the previous section. Periodic boundary condition is adopted, and the following initial condition is chosen:

$$\rho_j(1) = \rho_j(0) = \begin{cases} \rho_0; & j \neq \frac{M}{2}, \frac{M}{2}+1 \\ \rho_0 - \sigma; & j = \frac{M}{2} \\ \rho_0 + \sigma; & j = \frac{M}{2}+1 \end{cases}$$

where, $\sigma = 0.1$ is the initial disturbance and M is the total number of lattice sites taken as 100.

As discussed in the previous section that the mKdV equation exists only for $0 \leq \gamma < f(\alpha, p)$, we will discuss our numerical results for two different range of γ as follows:

Case 1: $\gamma < f(\alpha, p)$

Figure 3 depicts the effect of parameter p representing the drivers' characteristics on the simulation results of spatio-temporal evolution of density after 2×10^4 time steps for smaller rate of passing $\gamma = 0.05$. It is clear from Fig. 3a–c that a small disturbance in the uniform density leads to the kink–antikink soliton representing stop-and-go waves which propagates in the backward direction. Due to this, initial homogeneous
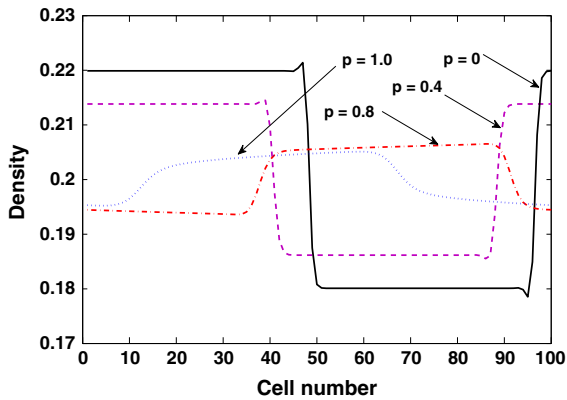
Fig. 4 Density profiles at time $t = 20300$ when $\gamma = 0.05$, $\alpha = 0.1$, and $a = 3.2$ corresponding to the panel of Fig. 3

flow under a small amplitude disturbance evolves into congested flow as the stability condition is not satisfied. These stop-and-go density waves are expressed by the

kink–antikink soliton solution of the mKdV Eq. (23) discussed in Sect. 4. For $p = 1.0$, we entered into the stable region and a small amplitude perturbation to the homogeneous density dies out with time and stop-and-go wave disappears as shown in Fig. 3d. The traffic jam disappears, and flow becomes almost homogeneous at $p = 1.0$.

Figure 4 describes the density profile at time $t = 20300s$ corresponding to the panel of Fig. 3. On comparing the stop-and-go waves for different values of p, it can be easily depicted that the amplitude of stop-and-go waves gradually decreases with an increase in the value of p. This ensures the fact that the aggressive driver's characteristics have a positive effect on the stability of traffic flow and help in removing the traffic congestion in real traffic for smaller rate of passing. A natural consequence of these results is that aggressive driving characteristics are much more efficient than timid driving character-
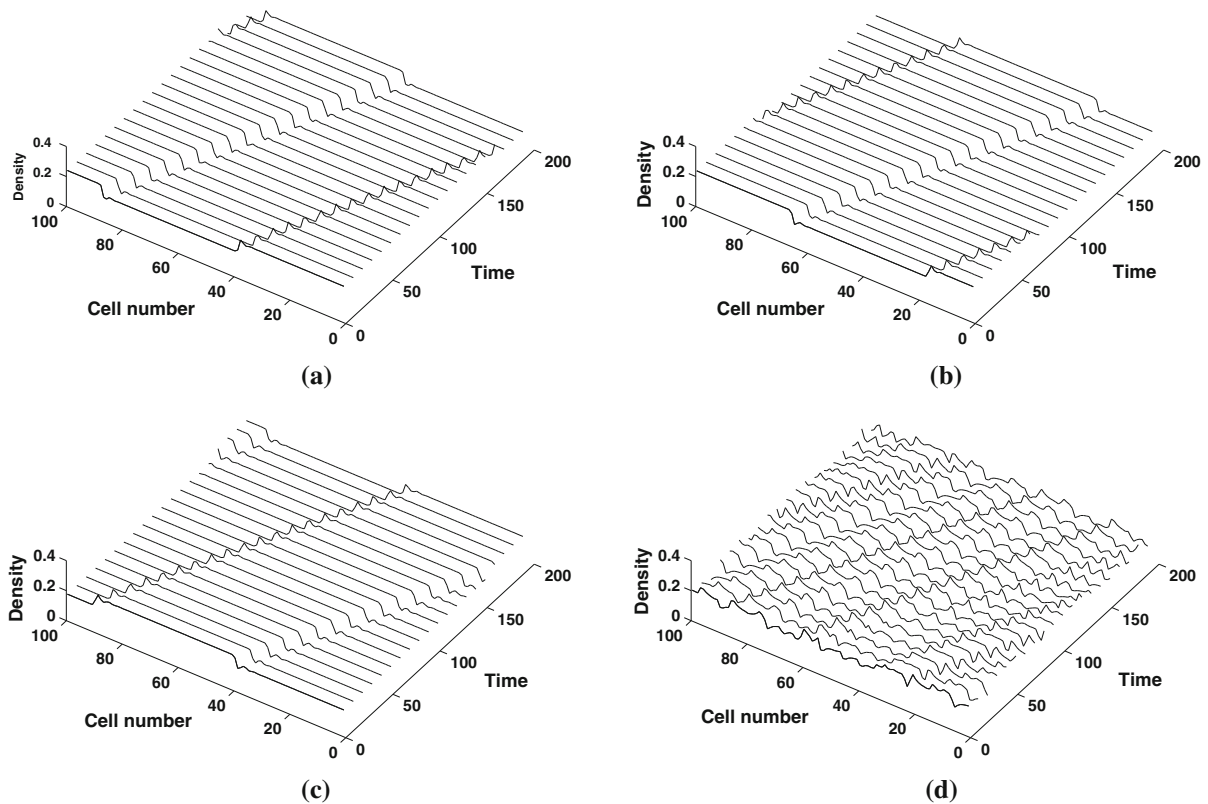

Fig. 5 Spatiotemporal evolutions of density when $\gamma = 0.3$, $\alpha = 0.1$, and $a = 3.5$ for **a** $p = 0$, **b** $p = 0.4$, **c** $p = 0.8$, and **d** $p = 1.0$, respectively
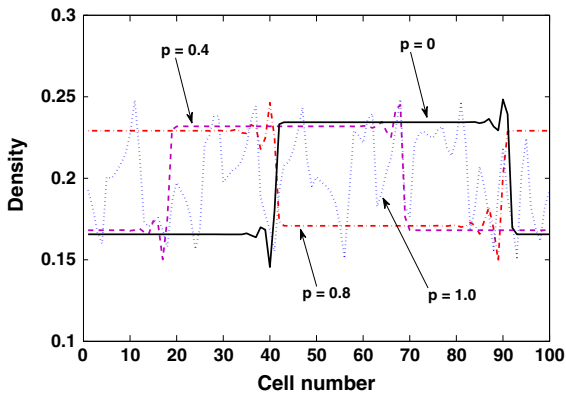
Fig. 6 Density profiles at time $t = 20300$ when $\gamma = 0.3$, $\alpha = 0.1$, and $a = 3.5$ corresponding to the panel of Fig. 5

istics in suppressing traffic congestion. Our simulation results are consistent with theoretical findings for $\gamma < f(\alpha, p)$.

Case 2: $\gamma \geq f(\alpha, p)$
Here, we further examine the effect of driver's characteristics on the traffic flow dynamics when passing is allowed at a significant rate ($\gamma = 0.3$). Figure 5 display the simulation results of spatiotemporal evolution of density after sufficiently long time, namely 2×10^4 time steps for the different values of p. It can be observed from Fig. 5 that the pattern of density profiles is different for larger value as compared to smaller values of p.

Patterns in Fig. 5a–c demonstrate that parallel to previous case of smaller rate of passing, initial small amplitude disturbance is amplified for smaller values of p leading to the kink–antikink soliton waves which propagates in the backward direction. While for higher values of p, the initial disturbance evolves in to chaotic waves. These waves band with one another, break up and propagates in the backward direction. So, It is evi-
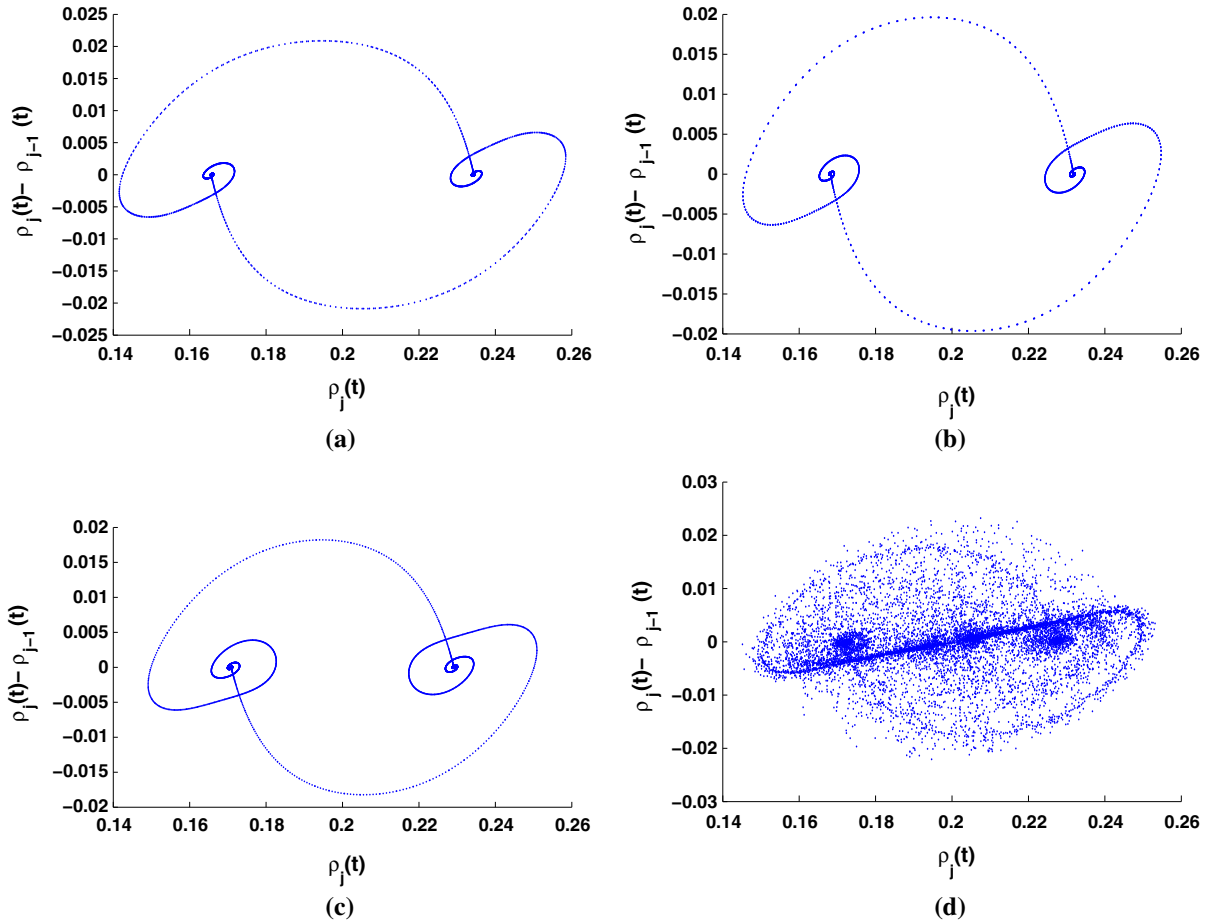

Fig. 7 Plots of density difference $\rho(t) - \rho(t-1)$ versus $\rho(t)$ when $\gamma = 0.3$, $\alpha = 0.1$, and $a = 3.5$ for **a** $p = 0$, **b** $p = 0.4$, **c** $p = 0.8$, and **d** $p = 1.0$, respectively

dent that the kink as well as the chaotic region exists in the unstable region on the phase plane which verifies the theoretical results presented in Sect. 4 and shown in Fig. 5.

To further analyze the effect of aggressive driver's characteristics on the steady-state density profiles, Fig. 6 describes the density profiles at time $t = 20,300$ s corresponding to the panel of Fig. 5. For $\gamma = 0.3$, the steady-state density profiles are expressed by kink-Bando waves till $a < \frac{3-2\alpha(2p-1)}{1-2f(\alpha,p)}$. Note that the amplitude of the density waves decreases with the increase in p which is similar to the results obtained in the previous case for small rate of passing. Further increase in p, the kink-Bando wave converts into chaotic wave. These numerical findings agree well with the theoretical results that for $a < a_c$, the traffic will be in kink phase and while a is greater than a_c, traffic flow will be chaotic. This result is quit interesting as the aggressive driver's characteristics on one hand plays a crucial role in stabilizing the traffic flow for smaller rate of passing while on the other hand above a critical value of p, their effect on traffic flow dynamics become adverse when passing is allowed at larger rate.

To further classify traffic states, the phase space plot of density difference $\rho(t) - \rho(t-1)$ against $\rho(t)$ at a fixed site is plotted for $t = 20,000$–$30,000$ in Fig. 7 corresponding to Fig. 6. The patterns shown in Fig. 7a–c exhibit the limit cycle which correspond to the periodic traffic behavior. The irregular traffic behavior which exhibits the behavior characteristic of chaos is shown by the set of dispersed points around a closed loop in the phase space plot in Fig. 7d. This validate the fact that as the drivers characteristics crosses the critical value, the traffic becomes irregular on a single-lane unidirectional highway when passing is allowed at higher rate. Therefore, from theoretical and simulation results, it is reasonable to conclude that traffic jam can efficiently suppressed by considering the driver's characteristics in a single-lane traffic system with passing.

6 Conclusion

A new lattice hydrodynamic model for traffic flow is developed to analyze the effect of driver's characteristics on the traffic flow dynamics when passing is allowed. The traffic behavior has been analyzed theoretically by the means of linear as well as nonlinear analysis and found that driver's characteristics play a

significant role in stabilizing the traffic flow on a single-lane highway with or without passing. Through nonlinear stability analysis, we derived the mKdV equation to describe the traffic jam near the critical point and obtained the condition for the existence of kink soliton solution of mKdV equation. The effect of different important parameters on the neutral stability curves and the coexisting curves are plotted and results are compared in the density-sensitivity phase space for smaller and larger rate of passing. It is observed that there exist two different regions kink jam and no jam on the phase plane for smaller rate of passing while an additional phase known as chaotic jam is seen when the rate of passing exceeds the critical value. It is concluded that in both the cases with or without passing, aggressive driver's characteristics are prompt to increases the stability of traffic flow significantly while the timid driver's characteristics have a opposite effect on the stability of traffic flow and increase congestion. The results obtained form numerical simulation are compared and found consistent with the theoretical findings. Finally, it is concluded that driver's characteristics has an significant impact on the stability of traffic flow on a single-lane traffic system with passing.

Though the present work is complete to describe the effect of driver's characteristics in traffic system with passing on a one-dimensional highway yet the proposed model should be extended to more realistic situation like multi-lane traffic system or a network. Moreover, the proposed results should also be validated by the experimental investigations on some real road which is our one of the future prospective.

Appendix

In this appendix, we give the expansion of each terms in Eq. (8) using Eqs. (17) and (18) to the fifth order of ϵ.***

$$\rho_j(t + \tau) = \rho_c + \epsilon R + \epsilon^2 (b\tau)\partial_X R$$
$$+ \frac{\epsilon^3}{2}(b\tau)^2\partial_X^2 R + \frac{\epsilon^4}{6}(b\tau)^3\partial_X^3 R + \epsilon^4\tau\partial_T R$$
$$+ \frac{\epsilon^5}{24}(b\tau)^4\partial_X^4 R + \epsilon^5 b\tau^2\partial_T\partial_X R. \qquad (32)$$
$$\rho_j(t + 2\tau) = \rho_c + \epsilon R + \epsilon^2 (2b\tau)\partial_X R$$
$$+ \frac{\epsilon^3}{2}(2b\tau)^2\partial_X^2 R$$

$$+ \frac{\epsilon^4}{6}(2b\tau)^3 \partial_X^3 R + \epsilon^4(2\tau)\partial_T R$$

$$+ \frac{\epsilon^5}{24}(2b\tau)^4 \partial_X^4 R + \epsilon^5(4b\tau^2)\partial_T \partial_X R. \quad (33)$$

$$\rho_{j+1}(t) = \rho_c + \epsilon R + \epsilon^2 \partial_X R + \frac{\epsilon^3}{2}\partial_X^2 R$$

$$+ \frac{\epsilon^4}{6}\partial_X^3 R + \frac{\epsilon^5}{24}\partial_X^4 R. \quad (34)$$

$$\rho_{j+1}(t+\tau) - 2\rho_j(t+\tau) + \rho_{j-1}(t+\tau)$$

$$= \epsilon^3 \partial_X^2 R + \epsilon^4(b\tau)\partial_X^3 R$$

$$+ \frac{\epsilon^5}{12}(1 + 6b^2\tau^2)\partial_X^4 R. \quad (35)$$

The expansion of optimal velocity function at the turning point is

$$V(\rho_j) = V(\rho_c) + V'(\rho_c)(\rho_j - \rho_c)$$

$$+ \frac{V'''(\rho_c)}{6}(\rho_j - \rho_c)^3. \quad (36)$$

$$V(\rho_{j+1}) = V(\rho_c) + V'(\rho_c)(\rho_{j+1} - \rho_c)$$

$$+ \frac{V'''(\rho_c)}{6}(\rho_{j+1} - \rho_c)^3. \quad (37)$$

Using Eqs. (36) and (37), we get

$$V(\rho_{j+1}) - V(\rho_j) = V'(\rho_c)\left[\epsilon^2 \partial_X R\right.$$

$$+ \frac{\epsilon^3}{2}\partial_X^2 R + \frac{\epsilon^4}{6}\partial_X^3 R + \frac{\epsilon^5}{24}\partial_X^4 R\right]$$

$$+ \frac{V'''(\rho_c)}{6}\left[\epsilon^4 \partial_X R^3 + \frac{\epsilon^5}{2}\partial_X^2 R^3\right]. \quad (38)$$

Some other important expansions are also computed using Eqs. (32)–(38) and are given as

$$V'(\rho_{j+1}(t))\tilde{\Delta}\rho_{j+1}(t) - V'(\rho_j(t))\tilde{\Delta}\rho_j(t)$$

$$= \frac{\epsilon^3}{2}(b\tau)V'(\rho_c)\partial_X^2 R + \frac{\epsilon^4}{2}(b^2\tau^2 + b\tau)V'(\rho_c)\partial_X^3 R$$

$$+ \epsilon^5 V'(\rho_c)\left[\tau\partial_T \partial_X R\right.$$

$$+ \frac{(4b\tau + 6b^2\tau^2 + 4b^3\tau^3)}{24}\partial_X^4 R\right]. \quad (39)$$

By inserting (32), (33), (35), (38), and (39) into Eq. (8), we obtain Eq. (19).

References

1. Chowdhury, D., Santen, L., Schadschneider, A.: Statistical physics of vehicular traffic and some related systems. Phys. Rep. **329**, 199–329 (2000)
2. Nagel, K., Schreckenberg, M.: A cellular automaton model for freeway traffic. J. Phys. **I**(2), 2221–2229 (1992)
3. Helbing, D.: Traffic and related self-driven many-particle systems. Rev. Mod. Phys. **73**, 1067 (2001)
4. Nagatani, T.: The physics of traffic jams. Rep. Prog. Phys. **65**, 1331–1386 (2002)
5. Bando, M., Hasebe, K., Nakayama, A., Shibata, A., Sugiyama, Y.: Dynamical model of traffic congestion and numerical simulation. Phys. Rev. E **51**, 1035 (1995)
6. Jiang, R., Wu, Q.S., Zhu, Z.J.: A new continuum model for traffic flow and numerical tests. Transp. Res. B Methodol. **36**, 405–419 (2002)
7. Gupta, A.K., Katiyar, V.K.: A new anisotropic continuum model for traffic flow. Phys. A **368**, 551–559 (2006)
8. Gupta, A.K., Katiyar, V.K.: Analyses of shock waves and jams in traffic flow. J. Phys. A Math. Gen. **38**, 4069–4083 (2005)
9. Gupta, A.K., Katiyar, V.K.: Phase transition of traffic states with on-ramp. Phys. A **371**, 674–682 (2006)
10. Nagatani, T.: Modified KdV equation for jamming transition in the continuum models of traffic. Phys. A **261**, 599–607 (1998)
11. Nagatani, T.: Chaotic jam and phase transition in traffic flow with passing. Phys. Rev. E **60**, 1535 (1999)
12. Ge, H.X., Cheng, R.J.: The backward looking effect in the lattice hydrodynamic model. Phys. A **387**, 6952–6958 (2008)
13. Peng, G.H., Cai, X.H., Cao, B.F., Liu, C.Q.: Non-lane-based lattice hydrodynamic model of traffic flow considering the lateral effects of the lane width. Phys. Lett. A **375**, 2823–2827 (2011)
14. Peng, G.H.: A new lattice model of traffic flow with the consideration of individual difference of anticipation driving behavior. Commun. Nonlinear Sci. Numer. Simul. **18**, 2801–2806 (2013)
15. Kang, Y.R., Sun, D.H.: Lattice hydrodynamic traffic flow model with explicit drivers physical delay. Nonlinear Dyn. **71**, 531–537 (2013)
16. Ge, H.X., Dai, S.Q., Xue, Y., Dong, L.Y.: Stabilization analysis and modified Korteweg–de Vries equation in a cooperative driving system. Phys. Rev. E **71**, 066119 (2005)
17. Ge, H.X.: The Korteweg–de Vries soliton in the lattice hydrodynamic model. Phys. A **388**, 1682–1686 (2009)
18. Ge, H.X., Cheng, R.J., Lei, L.: The theoretical analysis of the lattice hydrodynamic models for traffic flow theory. Phys. A **389**, 2825–2834 (2010)
19. Nagatani, T.: Jamming transitions and the modified Korteweg–de Vries equation in a two-lane traffic flow. Phys. A **265**, 297–310 (1999)
20. Peng, G.H.: A new lattice model of two-lane traffic flow with the consideration of optimal current difference. Commun. Nonlinear Sci. Numer. Simul. **18**, 559–566 (2013)
21. Peng, G.H.: A new lattice model of the traffic flow with the consideration of the driver anticipation effect in a two-lane system. Nonlinear Dyn. **73**, 1035–1043 (2013)

22. Gupta, A.K., Redhu, P.: Analyses of drivers anticipation effect in sensing relative flux in a new lattice model for two-lane traffic system. Phys. A **390**, 5622–5632 (2013)

23. Gupta, A.K., Redhu, P.: Analyses of the drivers anticipation effect in a new lattice hydrodynamic traffic flow model with passing. Nonlinear Dyn. **76**, 1001–1011 (2014)

24. Zhang, M., Sun, D.H., Tian, C.: An extended two-lane traffic flow lattice model with drivers delay time. Nonlinear Dyn. **77**, 839–847 (2014)

25. Peng, G.H., Cai, X.H., Liu, C.Q., Cao, B.F.: A new lattice model of traffic flow with the consideration of the drivers forecast effects. Phys. Lett. A **375**, 2153–2157 (2011)

26. Peng, G.H., Nie, F.Y., Cao, B.F., Liu, C.Q.: A drivers memory lattice model of traffic flow and its numerical simulation. Nonlinear Dyn. **67**, 1811–1815 (2012)

27. Sharma, S.: Lattice hydrodynamic modeling of two-lane traffic flow with timid and aggressive driving behavior. Phys. A **421**, 401–411 (2015)

28. Sharma, S.: Effect of drivers anticipation in a new two-lane lattice model with the consideration of optimal current difference. Nonlinear Dyn. **81**, 991–1003 (2015)